

# Krisynomycins, Imipenem Potentiators against Methicillin-Resistant *Staphylococcus aureus*, Produced by *Streptomyces canus*

Mercedes Pérez-Bonilla,\* Daniel Oves-Costales, Ignacio González, Mercedes de la Cruz, Jesús Martín, Francisca Vicente, Olga Genilloud, and Fernando Reyes\*



Cite This: <https://dx.doi.org/10.1021/acs.jnatprod.0c00294>



Read Online

ACCESS |



Metrics & More



Article Recommendations



Supporting Information

**ABSTRACT:** A reinvestigation of the acetone extract of the strain CA-091830 of *Streptomyces canus*, producer of the imipenem potentiator krisynomycin, resulted in the isolation of two additional analogues, krisynomycins B (1) and C (2), with different chlorination patterns. Genome sequencing of the strain followed by detailed bioinformatics analysis led to the identification of the corresponding biosynthetic gene cluster (BGC) of this cyclic nonribosomal peptide family. The planar structure of the new molecules was determined using HRMS, ESI-qTOF-MS/MS, and 1D and 2D NMR data. Their absolute configuration was proposed using a combination of Marfey's and bioinformatic BGC analyses. The krisynomycins displayed weak to negligible antibiotic activity against methicillin-resistant *Staphylococcus aureus* (MRSA), which was significantly enhanced when tested in combination with sublethal concentrations of imipenem. The halogenation pattern plays a key role in the antimicrobial activity and imipenem-potentiating effects of the compounds, with molecules having a higher number of chlorine atoms potentiating the effect of imipenem at lower doses.



Antimicrobial resistance (AMR) threatens the effective prevention and treatment of an ever-increasing range of infections caused by bacteria, parasites, viruses, and fungi.<sup>1</sup> Although AMR occurs naturally over time, this process is being accelerated by the misuse and overuse of antibiotics, as well as poor infection prevention and control.<sup>1,2</sup> It has been estimated that AMR will cause around 10 million deaths a year by 2050, being the major cause of death in comparison with other major health problems, such as cancer.<sup>3</sup>

Nature has been historically the source of a considerable number of drugs developed from microorganisms of varied environments.<sup>4,5</sup> In fact, actinomycetes, and *Streptomyces* in particular, have been for decades one of the most significant sources for the discovery of new antibiotics, with a number of drugs successfully introduced in the market and still used today in clinical practice.<sup>6,7</sup>

Peptides, and notably natural cyclic peptides such as vancomycin, daptomycin, and polymyxin B, have gained special attention due to their remarkable variety of structures and valuable functions. To date, more than 40 cyclic peptide drugs are currently on the market, and approximately one new cyclopeptide drug enters the market annually on average.<sup>8</sup>

Methicillin-resistant *Staphylococcus aureus* (MRSA) is a common cause of infection in hospitals and the community.  $\beta$ -Lactam antibiotics are the most successful chemical class of antibiotics used to treat infections in humans.<sup>9</sup> However, the acquisition of a non-native gene encoding a  $\beta$ -lactam-

insensitive penicillin-binding protein (PBP2a) allows MRSA to proliferate in the presence of typically inhibitory concentrations of  $\beta$ -lactam antibiotics.<sup>10</sup> Nonetheless, those compounds that interfere with the stability of PBP2a render MRSA susceptible to  $\beta$ -lactam antibiotics. Consequently, another strategy to address emerging resistance is the identification of molecules that could potentiate or enhance the activity of existing antibacterial agents. Probably, the best known combinations with  $\beta$ -lactam antibiotics are the drugs amoxicillin-clavulanic acid, ampicillin-sulbactam, and piperacillin-tazobactam, but other molecules that potentiate the  $\beta$ -lactam antibiotic activity have also been reported.<sup>11</sup> The cyclic depsipeptide krisynomycin and the lipoglycopeptide actinocarbasin are also among the compounds that potentiate the activity of imipenem against the MRSA strain COL.<sup>12</sup> Other imipenem potentiators against MRSA isolated from microorganisms are cyslabdan, cyslabdans B and C,<sup>13,14</sup> and the xanthoradones A, B, and C.<sup>15</sup>

Received: March 17, 2020

Table 1.  $^1\text{H}$  (500 MHz) and  $^{13}\text{C}$  (125 MHz) NMR Data of Compounds 1–3 in  $\text{DMSO-}d_6$ 

residue	position	1		2		3	
		$\delta_{\text{C}}$ , mult. <sup>a,b</sup>	$\delta_{\text{H}}$ , mult. (J in Hz)	$\delta_{\text{C}}$ , mult. <sup>a,b</sup>	$\delta_{\text{H}}$ , mult. (J in Hz)	$\delta_{\text{C}}$ , mult.	$\delta_{\text{H}}$ , mult. (J in Hz)
malonic acid	1	169.3, C				170.3, C	
	2	42.1, CH <sub>2</sub>	3.18, d (5.5)	43.4, CH <sub>2</sub>	3.18, br s	43.1, CH <sub>2</sub>	3.09, m
	3	165.2, C				166.5, C	
Ala	4	171.9, C		171.9, C		172.3, C	
	5	48.0, CH	4.39, m	49.3, CH	4.38, m	48.3, CH	4.33, m
Val 1	NH		8.26 d (7.4)		8.27, m		8.44, m
	6	18.0, CH <sub>3</sub>	1.20, d (7.1)	19.4, CH <sub>3</sub>	1.20, d (7.0)	18.1, CH <sub>3</sub>	1.21, d (7.0)
	7	170.5, C				171.0, C	
Ser 1	8	57.3, CH	4.20, m	58.6, CH	4.21, m	57.6, CH	4.19, m
	NH		7.88, d (8.6)		7.89, m		8.12, m
	9	30.4, CH	2.00, m	31.7, CH	2.00, m	30.4, CH	2.01, m
	10	18.8, CH <sub>3</sub>	0.84, m	20.2, CH <sub>3</sub>	0.82, m	19.2, CH <sub>3</sub>	0.81, m
	11	17.7, CH <sub>3</sub>	0.83, m	19.1, CH <sub>3</sub>	0.83, m	18.0, CH <sub>3</sub>	0.82, m
Cya	12	167.7, C				168.0, C	
	13	51.4, CH	4.48, dd (11.9, 7.1)	52.7, CH	4.49, m	51.7, CH	4.50, m
	NH		8.04, d (7.1)		8.05, d (7.0)		8.05, d (6.8)
Pro	14	63.5, CH <sub>2</sub>	4.16, m	64.8, CH <sub>2</sub>	4.17, m	63.7, CH <sub>2</sub>	4.18, m
			4.10, m		4.10, m		4.08, m
	15	171.2, C				171.3, C	
Trp	16	47.2, CH	5.17, ddd (12.7, 7.5, 5.3)	48.6, CH	5.16, m	47.5, CH	5.13, m
	NH		8.42, d (7.5)		8.41, d (7.6)		8.37, d (7.3)
	17	52.6, CH <sub>2</sub>	3.42, m	54.0, CH <sub>2</sub>	3.42, m	52.8, CH <sub>2</sub>	<sup>d</sup>
prenyl Trp			2.90, br d (12.7)		2.90, m		2.95, m
	18	173.7, C				173.7, C	
	19	61.0, CH	4.42, m	62.3, CH	4.42, m	61.2, CH	4.39, m
	20	29.2, CH <sub>2</sub>	1.95, m	30.6, CH <sub>2</sub>	1.96, m	29.4, CH <sub>2</sub>	1.95, m
			1.51, m		1.52, m		1.48, m
	21	23.7, CH <sub>2</sub>	1.81, m	25.1, CH <sub>2</sub>	1.82, m	23.9, CH <sub>2</sub>	1.80, m
			1.48, m		1.50, m		1.45, m
prenyl Trp	22	47.3, CH <sub>2</sub>	4.26, m	48.7, CH <sub>2</sub>	4.23, m	47.5, CH <sub>2</sub>	4.20, m
			3.92, m		3.91, m		3.91, m
	23	171.7, C				171.7, C	
	24	56.7, CH	4.01, m	58.0, CH	4.01, m	56.8, CH	4.02, m
	NH		8.51, d (6.6)		8.57, d (6.8)		8.50, d (6.8)
	25	24.9, CH <sub>2</sub>	3.20, m	26.2, CH <sub>2</sub>	3.21, m	25.2, CH <sub>2</sub>	3.18, m
			2.92, br d (13.2)		2.91, m		2.91, m
	26	110.4, C		112.1, C		112.2, C	
	27	124.0, CH	7.34, d (2.2)	126.6, CH	7.43, br s	125.5, CH	7.41, br s
	NH (indole)		10.83, s		11.22, s		11.23, br s
prenyl Trp	28	135.9, C		132.7, C		132.8, C	
	29	111.2, CH	7.30, d (7.9)	115.6, C		115.8, C	
	30	120.7, CH	7.02, t (7.9)	121.5, CH	7.11, d (7.7)	120.4, CH	7.11, d (7.7)
	31	118.2, CH	6.91, t (7.9)	120.6, CH	6.91, t (7.7)	119.4, CH	6.91, t (7.7)
	32	117.9, CH	7.51, d (7.9)	118.4, CH	7.49, d (7.7)	117.4, CH	7.50, d (7.7)
	33	126.6, C		128.8, C		129.0, C	
	34	171.2, C				170.9, C	
	35	55.3, CH	4.38, m	56.7, CH	4.37, m	55.3, CH	4.38, m
	NH		7.66, d (8.6)		7.70, m		7.69, m
	36	27.9, CH <sub>2</sub>	3.68, m	29.3, CH <sub>2</sub>	3.69, m	28.2, CH <sub>2</sub>	3.63, br d (12.9)
prenyl Trp			3.01, dd (14.6, 11.1)		3.02, m		3.01, m
	37	110.2, C				112.1, C	
	38	125.7, CH	7.61, br s	127.0, CH	7.61, br s	127.3, CH	7.72, br s
	NH (indole)		10.71, s		10.72, s		10.99, br s
	39	136.8, C		133.2, C		133.4, C	
	40	109.4, CH	7.16, d (7.5)	110.7, CH	7.15d (7.2)	113.8, C	
	41	120.4, CH	6.92, t (7.5)	121.7, CH	6.92, t (7.2)	119.8, CH	7.03, d (7.8)
	42	118.4, CH	6.72, d (7.5)	119.7, CH	6.72, d (7.2)	119.5, CH	6.74, d (7.8)
	43	133.1, C		132.7, C		132.4, C	
	44	124.1, C		124.2, C		126.3, C	

Table 1. continued

residue	position	1		2		3	
		$\delta_C$ , mult. <sup>a,b</sup>	$\delta_H$ , mult. (J in Hz)	$\delta_C$ , mult. <sup>a,b</sup>	$\delta_H$ , mult. (J in Hz)	$\delta_C$ , mult.	$\delta_H$ , mult. (J in Hz)
Val 2	45	31.4, CH <sub>2</sub>	3.83, dd (15.1, 6.2) 3.72, m	32.8, CH <sub>2</sub>	3.83, dd (16.6, 6.2) 3.72, m	31.0, CH <sub>2</sub>	3.82, m 3.72, m
	46	123.9, CH	5.33, m	125.2, CH	5.33, m	123.5, CH	5.30, m
	47	130.9, C		131.0, C		131.8, C	
	48	17.6, CH <sub>3</sub>	1.70, s	19.0, CH <sub>3</sub>	1.70, s	17.9, CH <sub>3</sub>	1.71, s
	49	25.3, CH <sub>3</sub>	1.70, s	26.7, CH <sub>3</sub>	1.70, s	25.5, CH <sub>3</sub>	1.71, s
	50	170.7, C		170.9, C		171.3, C	
	51	59.5, CH	4.08, m	60.8, CH	4.09, m	59.6, CH	4.09, m
	NH		7.42, d (8.6)		7.41, m		7.48, m
	52	30.4, CH	1.98, m	31.7, CH	1.98, m	30.6, CH	2.00, m
	53	18.8, CH <sub>3</sub>	0.84, m	20.4, CH <sub>3</sub>	0.87, m	19.1, CH <sub>3</sub>	0.84, m
Leu	54	17.9, CH <sub>3</sub>	0.81, m	19.5, CH <sub>3</sub>	0.81, m	18.3, CH <sub>3</sub>	0.78, m
	55	171.8, C				172.1, C	
	56	50.8, CH	4.38, m	52.2, CH	4.38, m	51.1, CH	4.37, m
	NH		7.51, m		7.51, m		7.55, d (7.2)
	57	39.8, CH <sub>2</sub>	1.50, m	41.2, CH <sub>2</sub>	1.50, m	<sup>c</sup> , CH <sub>2</sub>	1.49, m
	58	23.9, CH	1.58, m	25.3, CH	1.59, m	24.1, CH	1.57, m
	59	21.1, CH <sub>3</sub>	0.81, m	22.5, CH <sub>3</sub>	0.82, m	21.4, CH <sub>3</sub>	0.81, m
	60	22.7, CH <sub>3</sub>	0.84, m	24.1, CH <sub>3</sub>	0.85, m	22.9, CH <sub>3</sub>	0.84, m
Ser 2	61	169.3, C		169.2, C		169.5, C	
	62	55.1, CH	4.15, m	56.4, CH	4.16, m	55.2, CH	4.17, m
	NH		7.55, m		7.58, m		7.67, m
	63	60.2, CH <sub>2</sub>	3.78, m 3.72, m	61.6, CH <sub>2</sub>	3.78, m 3.73, m	60.4, CH <sub>2</sub>	3.77, m 3.72, m
	OH		4.95, br s		4.95, br s		4.97, m

<sup>a</sup>CH and CH<sub>2</sub> were assigned based on HSQC correlations. <sup>b</sup>Quaternary carbons were assigned based on HMBC correlations. <sup>c</sup>Obscured by solvent peak. <sup>d</sup>Obscured by water peak.

The planar structure of krisynomycin has been previously reported,<sup>12</sup> but no isolation procedures or spectroscopic data have been so far disclosed for this molecule. The krisynomycin producer strain CA-091830, available from MEDINA's collection, was used for cultivation and isolation of this compound and other congeners. LC-HRMS analysis of the extract revealed the presence of krisynomycin and two new structurally related components in the chromatographic profile, which prompted a more detailed investigation of its composition. Extraction of the culture broth followed by a chromatographic fractionation of the extract led to the isolation of the new krisynomycins B and C (**1** and **2**) and krisynomycin (**3**). Recent advances in biosynthetic gene cluster (BGC) analysis are providing very valuable information from the assembly line enzymology of natural products, such as polyketides and nonribosomal peptides, which is effectively used to support the determination of the stereochemistry of these compounds.<sup>16,17</sup> As an example, the stereochemistry of the lipodepsipeptide BII-Rafflesfungin was determined using the combined information obtained from Marfey's analysis and the BGC.<sup>17</sup> Hence, a bioinformatic analysis of the krisynomycin BGC was employed to support the proposed absolute configuration of the krisynomycin family. Structural elucidation, including the absolute configuration of the three compounds using a combination of NMR spectroscopy and Marfey's and BGC analyses together with their activity as imipenem potentiators, is reported.

## RESULTS AND DISCUSSION

**Structural Elucidation of the Planar Structure of Krisynomycins.** Compound **1** was obtained as a white

amorphous solid. A molecular formula of C<sub>63</sub>H<sub>86</sub>N<sub>12</sub>O<sub>18</sub>S was deduced from the (+)-ESI-TOF analysis ([M + H]<sup>+</sup> 1331.5981,  $\Delta$  +0.0004). The <sup>1</sup>H NMR spectrum of **1** in DMSO-*d*<sub>6</sub> displayed signals that were attributable to a peptide, including amide hydrogens (N–H) around 8 ppm and signals of  $\alpha$ -amino acid hydrogens between 4 and 5 ppm (Table 1). Interpretation of the 2D NMR data (COSY, TOCSY, HSQC, and HMBC) allowed us to identify the presence of Ala, 2 × Val, 2 × Ser, Cya, Pro, Trp, Prenyl-Trp, and Leu residues as well as the cyclic nature of the depsipeptide, which was confirmed later by HRMS fragmentation. In addition to these common amino acids, a signal at  $\delta_H$  3.18 (H<sub>2</sub>-2) assigned to a methylene group coupled to two carbonyls at  $\delta_C$  169.3 (C-1) and 165.2 (C-3) in the HMBC spectrum accounted for the presence of a malonic acid residue. A characteristic feature of the compound was an olefinic hydrogen at  $\delta_H$  5.33 (m, H-46) in the <sup>1</sup>H NMR spectrum, attributed to the presence of a trisubstituted double bond, which was also evidenced by the sp<sup>2</sup> signals at  $\delta_C$  123.9 (C-46) and 130.9 (C-47) in the <sup>13</sup>C NMR spectrum. Signals of two singlet methyl groups at  $\delta_H$  1.70 (6H, s, H<sub>3</sub>-48 and H<sub>3</sub>-49) suggested that the double bond was substituted by two methyl groups. Finally, the methylene hydrogens at  $\delta_H$  3.72 and 3.83 (H<sub>2</sub>-45), coupled in the COSY spectrum to H-46, corroborated the presence of a prenyl unit. Correlations in the HMBC spectrum between H<sub>2</sub>-45 and the carbons C-42, C-43, C-46, and C-47 indicated that the prenyl unit was linked to C-43 of one of the tryptophan residues.

The connections between the different amino acids were first inferred from HMBC correlations involving the NH hydrogens of the peptidic bonds (Figure 1). HRMS fragmentation data additionally supported the amino acid

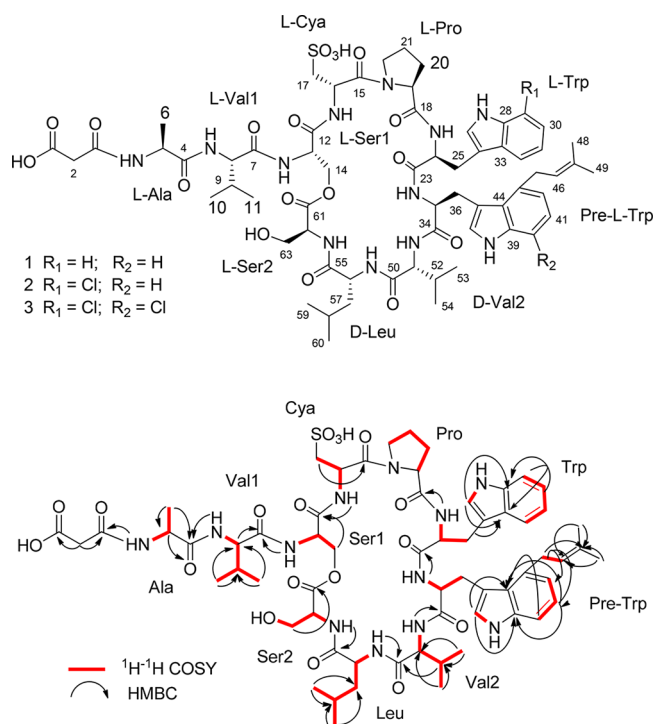


**Figure 1.**  $^1\text{H}$ – $^1\text{H}$  COSY and key HMBC correlations for **1**.

sequence. Hydrolysis of **1** under basic conditions yielded the linear peptide (Figure 2). Acquisition of the MS<sup>2</sup> spectrum of the protonated linear peptide ( $[\text{M} + \text{H}]^+$  1349.6058) led to the identification of several key fragments that confirmed the structure proposed by NMR analysis. The first fragmentation originated the ion at  $m/z$  1244.5665 ( $[\text{M} + \text{H}]^+$ ) accounting for the residue Malonate-Ala-Val-Ser-Cya-Pro-Trp-Pre-Trp-Val-Leu by loss of the terminal Ser amino acid. Subsequent losses of Leu and Val originated the fragments at  $m/z$  1131.4823 and 1032.4096. Cleavage of the amide bond between both Trp units and loss of the Pre-Trp residue originated the ion at  $m/z$  778.2696 ( $[\text{M} + \text{H}]^+$ ). The rest of the peptide could be sequenced by successive losses of the amino acids Trp, Pro, and Cya, originating the ions at  $m/z$  592.1910, 495.1361, and 344.1475, respectively. The amino acid sequence was also confirmed by the ions at  $m/z$  855.4751, 758.4234, 572.3419, 318.2045, and 219.1348 by successive cleavage of the amide bonds between the amino acids Pro-Trp-Pre-Trp-Val-Leu-Ser as indicated in Figure 2. Compound **1** was named krisynomycin B.

Compound **2** was obtained as a white amorphous solid. A molecular formula of C<sub>63</sub>H<sub>85</sub>ClN<sub>12</sub>O<sub>18</sub>S was deduced from the (+)-ESI-TOF analysis ( $[\text{M} + \text{H}]^+$  1365.5609,  $\Delta$  –0.0022), suggesting that **2** was a chlorinated version of **1**. The major difference between the  $^1\text{H}$  NMR data of both compounds was the absence of an aromatic hydrogen in one of the Trp residues. The absence of the signal corresponding to H-29, the multiplicity observed for H-30 to H-32 in **2**, and correlations observed in the COSY spectrum between H-30/H-31 and H-31/H-32 located the chlorine atom at C-29 of the Trp residue (Figure S1), whose  $^{13}\text{C}$  signal did not display correlations in the HSQC spectrum. Consequently, C-29 experienced a small downfield shift to  $\delta_{\text{C}}$  115.6 (Table 1). Compound **2** was named krisynomycin C.

Krisynomycin (**3**) was also obtained as a white amorphous solid. A molecular formula of C<sub>63</sub>H<sub>84</sub>Cl<sub>2</sub>N<sub>12</sub>O<sub>18</sub>S was assigned

based on its (+)-ESI-TOF analysis ( $[\text{M} + \text{H}]^+$  1399.5208,  $\Delta$  –0.0011). Its NMR data were similar to those of compound **2**, with the major difference being the disappearance of the signal of the aromatic hydrogen H-40 in the Prenyl-Trp residue and a change in the multiplicity of H-41 from triplet to doublet with respect to **1** and **2**. These changes were in agreement with the location of the additional chlorine atom in krisynomycin at C-40. Consequently, this carbon underwent a small downfield shift to 113.8 ppm (Table 1). COSY and HMBC correlations corroborated the position of this second chlorine atom at C-40 of the Prenyl-Trp residue (Figure S2). NMR data confirmed the planar structure previously described for krisynomycin.<sup>12</sup>

**Marfey's Analysis.** Once the planar structures of the three compounds were established, Marfey's analysis was used to determine the absolute configuration of each amino acid residue.<sup>18</sup> Acid hydrolysis of the cyclic depsipeptides followed by LC-MS analysis of the hydrolysates after derivatization with *N*-(2,4-dinitro-5-fluorophenyl)-D/L-valinamide (D/L-FDVA, Marfey's reagent) and comparison with the retention times and mass spectra obtained for standards revealed the presence of L-Ala, D-Val, L-Val, L-Cya, L-Pro, two units of L-Ser, and D-Leu (Figures S4–S7). The determination of the absolute configuration of the Trp-containing units was unsuccessful, even if phenol<sup>19</sup> or thioglycolic acid<sup>20,21</sup> was added as protective agent in the acid hydrolysis to prevent the degradation of tryptophan. Moreover, the presence of both D- and L-Val was detected, preventing the determination of the absolute configuration of the krisynomycins due to the location of the two residues of this amino acid in the three molecules.

**In Silico Analysis of the Krisynomycins' Biosynthetic Gene Cluster.** The genome of *Streptomyces canus* CA-091830 was sequenced and assembled employing a combination of PacBio and Illumina NovaSeq 6000 (Macrogen, Seoul, South Korea). All contigs were analyzed using antiSMASH,<sup>22</sup> revealing 26 regions potentially encoding secondary metabolite gene clusters. The krisynomycins are cyclic nonribosomal depsipeptides displaying three specific features, which we envisioned could guide us in the identification of their BGC: prenylation of one Trp residue at position C-43, chlorination of one or two Trp residues at positions C-29/C-40, and the presence of Cya as one of the units in the NRPS-synthesized backbone. Additionally, analysis of the peptide backbone indicated that the NRPS system should comprise 10 modules, assuming a canonical sequential assembly of the amino acid units.<sup>23</sup> Careful examination of the NRPS-containing regions identified by antiSMASH allowed us to identify a single BGC spanning 50 kb, which fulfilled the above requirements (Figure 3 and Table S7). Thus, *kriC* encodes a pyridoxal-phosphate-dependent enzyme (pfam00291), which shows homology to ANS62969.1 (47% identity, 57% similarity) and AAM06667.1 (37% identity, 51% similarity), two biochemically characterized cysteate synthases from *Streptomyces lincolnensis* and *Methanosarcina acetivorans*, respectively,<sup>24,25</sup> and therefore is proposed to catalyze the formation of cysteate from *O*-phospho-L-serine and sulfite. *kriE* encodes a FADH<sub>2</sub>-dependent (pfam04820) tryptophan halogenase, which shows high homology (64% identity, 77% similarity) to RebH, the biochemically characterized tryptophan 7-halogenase from rebeccamycin biosynthesis.<sup>26</sup> Unlike as is seen for the rebeccamycin cluster, a flavin reductase to generate FADH<sub>2</sub> cannot be found within the krisynomycin BGC putative boundaries. Presumably one of the five flavin reductases that we have identified, encoded elsewhere in the genome of

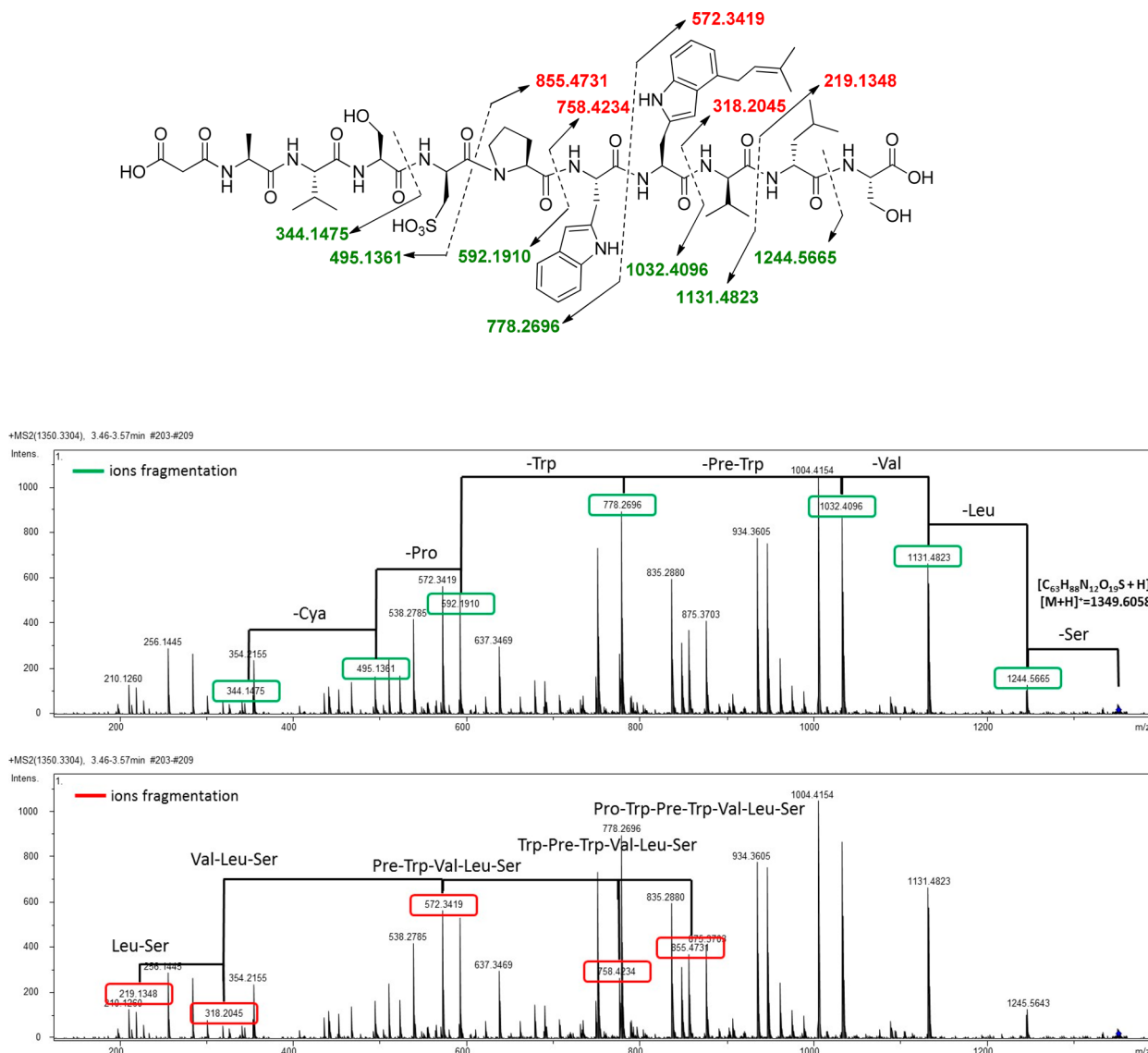


Figure 2. Fragments observed for 1 by MS<sup>n</sup>.

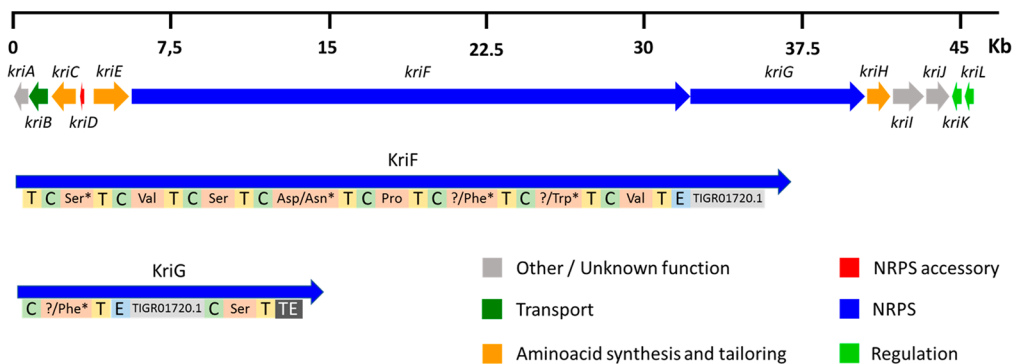
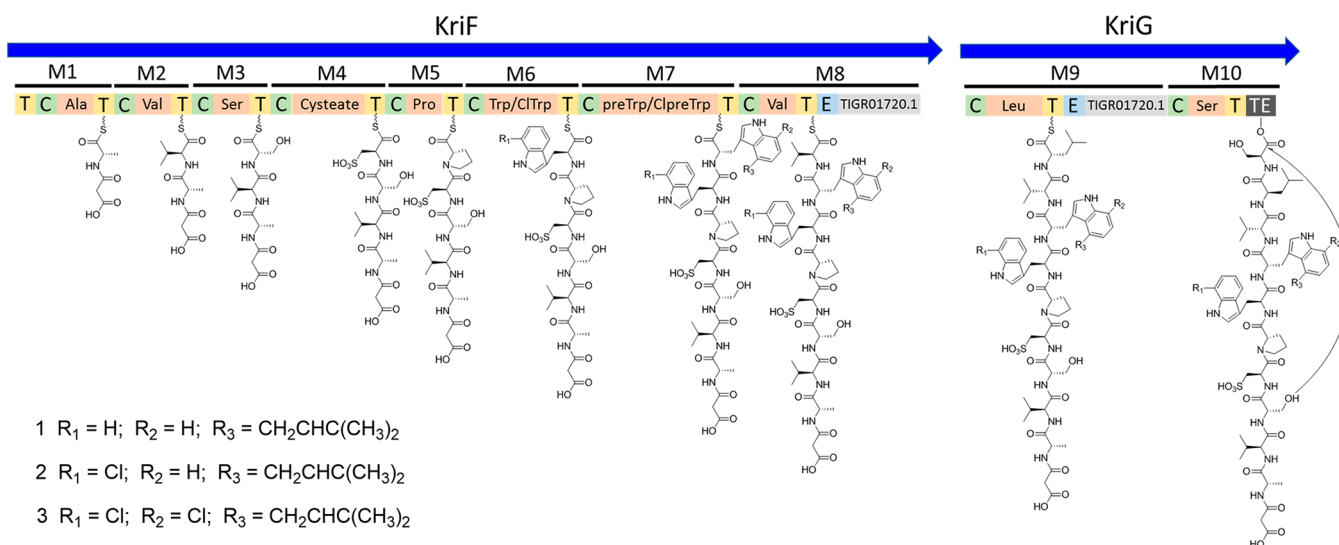


Figure 3. Putative krisynomycins BGC and domain organization of the NRPS proteins. The adenylation domains are labeled with the antiSMASH and PRISM amino acid specificity prediction. Asterisks indicate a mismatch between the prediction and the amino acids incorporated into the compounds.

*Streptomyces canus* CA-091830, is responsible for the NADH-dependent reduction of FAD to provide the FADH<sub>2</sub> for the halogenation at C-7 of L-tryptophan. *kriH* encodes a 370 aa protein that belongs to the ABBA-type family of aromatic prenyltransferases. Actinobacterial prenyltransferases catalyzing

the prenylation of L-tryptophan at different positions have been described recently, including IsaA from *Streptomyces* sp. MBT28, which catalyzes the addition of a prenyl unit to position C-7 of L-Trp,<sup>27</sup> IptA from *Streptomyces* sp. SN-593, which catalyzes prenylation of L-Trp at C-6,<sup>28</sup> SCO7467 from



**Figure 4.** Proposed biosynthesis of the krisynomycins.

*Streptomyces coelicolor* A3(2), which catalyzes prenylation of L-Trp at C-5,<sup>29</sup> and CymD from *Salinispora arenicola*, which promotes the addition of a prenyl unit to position N-1 of L-Trp.<sup>30</sup> Fungal prenyltransferases catalyzing prenylation at C-4 of L-Trp and indole derivatives have also been characterized.<sup>31,32</sup> However, to the best of our knowledge, no bacterial prenyltransferase catalyzing the transfer of a prenyl unit to position C-4 of L-Trp has been described. KriH shows relatively low levels of homology to IsaA (23% identity, 35% similarity), IptA (21% identity, 37% similarity), SCO7467 (24% identity, 38% similarity), or FgaPT2 (11% identity, 24% similarity). It could be hypothesized that KriH catalyzes prenylation of L-tryptophan at C-4 to afford 4-prenyl-L-Trp, which could then be employed by the NRPS to generate the krisynomycins. 4-Prenyl-L-Trp might also be the substrate for KriE, thus generating 7-chloro-4-prenyl-L-Trp, which in turn could be used by the NRPS to afford krisynomycin. Additionally, KriE is likely to be able to employ L-Trp as substrate to afford 7-chloro-L-Trp, which would be required in the biosynthesis of krisynomycin and krisynomycin C. Alternatively, chlorination of L-Trp by KriE at C-7 might take place prior to the prenylation at C-4 catalyzed by KriH (Figure S8).

On the other hand, *kriF* and *kriG* encode two multimodular nonribosomal peptide synthetases encompassing 10 modules. Adenylation domain specificity was analyzed using both antiSMASH<sup>22</sup> and PRISM,<sup>33</sup> which predicted a peptide backbone comprising Ser, Val, Ser, Asp/Asn, Pro, unknown/Phe, unknown/Trp, Val, unknown/Phe, and Ser (Figure 3). Several discrepancies are found between the bioinformatic prediction and the structures of krisynomycins. The adenylation domain of module 1 is predicted to incorporate Ser, but instead the Ala residue was found at the N-terminus in all three krisynomycins. The prediction for the adenylation domain of module 4 is either Asp (antiSMASH) or Asn (PRISM), yet Cya is selected in all cases. No prediction is obtained for the adenylation domains of modules 6 and 7 by antiSMASH, and Phe and Trp are suggested by PRISM. It is likely that these two adenylation domains have a relaxed substrate specificity, and so module 6 might be able to load L-tryptophan (to afford krisynomycin B) or 7-chloro-L-tryptophan (to generate krisynomycin and krisynomycin C),

whereas module 7 might be able to load 4-prenyl-L-tryptophan (to afford krisynomycins B and C) or 7-chloro-4-prenyl-L-tryptophan (to generate krisynomycin). Finally, the adenylation domain of module 9 is predicted to incorporate Phe (PRISM), but instead the Leu residue was found in all krisynomycins. These mismatches between the bioinformatic predictions and the substrates actually selected by the adenylation domains stress the importance of further refinement of the available domain-analysis tools.

Importantly, two epimerization domains are found in modules 8 and 9, which is in agreement with both the antiSMASH analysis and a phylogenetic study of the amino acid sequences from the condensation domains, which indicates that the C-domains from modules 9 and 10 belong to the <sup>D</sup>C<sub>L</sub> subtype<sup>34</sup> and therefore catalyze the condensation of an upstream T-loaded D-amino acid with a downstream T-loaded L-amino acid. All remaining C-domains belong to the <sup>L</sup>C<sub>L</sub> subtype. Taking these observations together and the MS/MS, NMR, and Marfey's analysis data, revealing the presence of both D- and L-Val, we propose the amino acid sequence L-Ala, L-Val, L-Ser, L-Cya, L-Pro, L-Trp/7-Cl-L-Trp, 4-prenyl-L-Trp/7-Cl-4-prenyl-L-Trp, D-Val, D-Leu, L-Ser as the backbone synthesized by the NRPS and found in the structures of the three krisynomycins (Figure 4). It is worth noting that the hypothetical krisynomycin derivative that would be obtained with the selection and loading of L-Trp and 7-Cl-4-prenyl-L-Trp by modules 6 and 7, respectively, has not been isolated nor even detected by LC-MS in the culture extracts.

Finally, the T-<sup>L</sup>C<sub>L</sub> didomain from module 1 is likely to be involved in the condensation of a malonic acid unit into the N-terminus alanine residue. It could be speculated that the malonate could be ACP-, CoA-, or AMP-mediated transferred into the first T domain from module 1 and then condensed with the free NH<sub>2</sub> group of the alanine residue by the <sup>L</sup>C<sub>L</sub> domain from the same module.

**Antibacterial Activity.** As krisynomycin has been previously reported as an imipenem synergistic compound,<sup>12</sup> the efficiency of the combined treatment of krisynomycins B and C together with imipenem against MRSA was also investigated using the liquid microdilution method. Neither of the krisynomycins B and C showed antibacterial activity when tested alone (MICs above 128 μg/mL, Table 2) compared to

**Table 2. Potentiation of Antimicrobial Activity against MRSA MB5393 by Krisynomycins 1–3<sup>a</sup>**

compound	MIC ( $\mu\text{g/mL}$ ) against MRSA MB5393			
	no imipenem	4 $\mu\text{g/mL}$ imipenem	2 $\mu\text{g/mL}$ imipenem	1 $\mu\text{g/mL}$ imipenem
krisynomycin B (1)	>128	8–16	16–32	16–32
krisynomycin C (2)	>128	2–4	4–8	4–8
krisynomycin (3)	16–32	0.25–0.5	0.5–1	0.5–1

<sup>a</sup>MIC imipenem = 16–32  $\mu\text{g/mL}$ .

the moderate activity shown by krisynomycin (MIC 16–32  $\mu\text{g/mL}$ , Table 2). However, all three compounds potentiated to a certain extent imipenem activity when methicillin-resistant *S. aureus* was exposed to different subinhibitory concentrations of the drug (4, 2, and 1  $\mu\text{g/mL}$ ) in the presence of different concentrations of krisynomycins. The combination of krisynomycin C and krisynomycin B with imipenem at 4  $\mu\text{g/mL}$  displayed an activity 8 to 32 times lower (MICs of 2–4 and 8–16  $\mu\text{g/mL}$ , respectively) than that of the mixture of krisynomycin with imipenem at 4  $\mu\text{g/mL}$  (MIC 0.25–0.5  $\mu\text{g/mL}$ ) (Figure S29). A similar behavior was observed when the compounds were combined with imipenem concentrations of 1 and 2  $\mu\text{g/mL}$  (Table 2). Our results therefore confirm that an increased number of chlorine atoms in the krisynomycin skeleton plays an important role on the potentiating effect of imipenem activity by the krisynomycin family. These findings are in line with the beneficial effects that the introduction of halogen atoms seem to have in the development of new drugs.<sup>35</sup>

In summary, krisynomycins are nonribosomal cyclic depsipeptides showing two specific structural features: prenylation and chlorination in the tryptophan amino acid units. Prenylation is a common modification of natural products from microbial and plant origin that contributes to their structural diversity. This functional group appears in many cases to provide a higher level of bioactivity in comparison with the nonprenylated precursors, often by increasing affinity for biological membranes and interactions with cellular targets.<sup>36</sup> As mentioned above, an explosion in the number of identified indole prenyltransferases has occurred in recent times,<sup>36,37</sup> although to the best of our knowledge this is the first time that a bacterial prenyltransferase catalyzing the addition of a prenyl unit to position C-4 of L-tryptophan is described.

An additional feature in the krisynomycins is the chlorination at position C-7 of L-tryptophan to produce 7-Cl-L-Trp and 7-Cl-4-prenyl-L-Trp in krisynomycin and krisynomycin C. Significantly, a large number of drugs and drug candidates in clinical development are halogenated structures. In fact, insertion of halogen atoms has been used in hit-to-lead or lead-to-drug optimization processes to increase membrane permeability and, therefore, improve the oral absorption of drug candidates. On one hand, previous studies have shown that halogen substituents influence the biomolecular interactions not only because of steric aspects but also as a result of the modification of thermodynamic parameters, with  $\Delta G$  being the parameter that best correlates with protein affinity ( $K_d$ ). Additionally, although sensible for the position of the halogen, dihalogenated peptides led to more stable complexes (lowest  $\Delta G$ ) with subsequent improvement in protein affinity.<sup>35,38</sup> A

number of halogenated metabolites have been isolated from living organisms, such as the antibiotics chloramphenicol and vancomycin, the antitumor agent rebeccamycin, whose biosynthesis also involves a regioselective enzymatic halogenation of tryptophan,<sup>39,40</sup> and the potential anticancer agent salinisporamide A.<sup>41</sup>

In conclusion, krisynomycins were shown to be novel natural products that act as synergistic agents of imipenem against MRSA. In addition to potentiating imipenem activity against MRSA, krisynomycins might also potentiate the antibacterial activity of other carbapenems and be effective against MRSA or other pathogenic clinical isolates. Consequently, they could constitute the starting point for the development of improved agents for combination therapies and expand the already broad active spectrum of imipenem.

## EXPERIMENTAL SECTION

**General Experimental Procedures.** Optical rotations were measured using a Jasco P-2000 polarimeter. UV spectra were obtained with an Agilent 1100 DAD. IR spectra were recorded on a JASCO FT/IR-4100 spectrometer equipped with a PIKE MIRacle single reflection ATR accessory. NMR spectra were recorded in DMSO-*d*<sub>6</sub> on a Bruker Avance III spectrometer (500 and 125 MHz for <sup>1</sup>H and <sup>13</sup>C NMR, respectively) equipped with a 1.7 mm TCI MicroCryoProbe (Bruker Biospin). Chemical shifts were reported in ppm using the signals of the residual solvent as internal reference ( $\delta_{\text{H}}$  2.50 and  $\delta_{\text{C}}$  39.51). LC-MS and LC-HRMS analyses were performed as previously described using an ionization voltage of 75 eV.<sup>42</sup>

**Microbial Isolation.** *Streptomyces canus* CA-091830 was isolated from a sand sample collected in 1997 in the Kalahari Desert in South Africa. The sand sample was subjected to a dry heat pretreatment at 100 °C for 1 h and serially diluted and plated on soil extract medium.<sup>43</sup>

**16S rRNA Sequencing and Phylogenetic Analysis.** The almost-complete 16S rRNA gene sequence (1514 bp) of strain CA-091830 was compared with those deposited in public databases and the EzBioCloud server (<https://www.ezbiocloud.net/><sup>44</sup>). The strain exhibited the highest identity (99.31%) with *Streptomyces canus* DSM 40017<sup>T</sup> (KQ948708), using EzBioCloud and GenBank sequence similarity searches and homology analysis.

Phylogenetic and molecular evolutionary analyses were conducted using MEGA version X.<sup>45</sup> Multiple alignment was carried out using CLUSTALX,<sup>46</sup> integrated in the software. The phylogenetic analysis, based on the neighbor-joining method<sup>47</sup> using matrix pairwise comparisons of sequences corrected with the Jukes and Cantor algorithm,<sup>48</sup> shows that the strain is closely related to the type strain *S. canus* DSM 40017<sup>T</sup> and can be proposed as a new strain of this species (Figure S9). The morphological and 16S rRNA gene sequence data were indicative that strain CA-091830 was a member of the genus *Streptomyces*, and the strain was referred to as *Streptomyces canus* CA-091830.

**Fermentation of the Producing Microorganism.** The first seed culture of the strain CA-091830 was prepared by inoculating 10 mL of seed medium, which consists of soluble starch (20 g/L), dextrose (10 g/L), NZ amine EKC (Sigma) (5 g/L), Difco beef extract (3 g/L), Bacto peptone (5 g/L), yeast extract (5 g/L), and CaCO<sub>3</sub> (1 g/L), adjusted to pH 7.0 with NaOH before addition of CaCO<sub>3</sub>, in a 40 mL tube with 0.5 mL of a frozen inoculum stock of the producing strain and incubating the tube at 28 °C with shaking at 220 rpm for 48 h. A second seed culture was prepared by inoculating 50 mL of seed medium in two 250 mL flasks with 2.5 mL of the first seed culture. A 5% aliquot of the second seed culture was transferred to each of the eight flasks (500 mL) containing 150 mL of the production CLA medium consisting of lactose monohydrate (Panreac 141375) (40 g/L), corn meal (Sigma-C6304) (40 g/L), and yeast autolysate (Sigma 43750) (5 g/L), adjusted to pH 7.0. The flasks were incubated at 28 °C for 7 days in a rotary shaker at 220 rpm and 70% humidity before harvesting.

**Isolation and Identification of Metabolites.** A culture (16 × 125 mL, 2 L) of the strain was obtained in CLA medium. Acetone was added to the fermentation flasks (1:1, 125 mL), and they were shaken in a Kühner at 220 rpm for 1 h. After that, the mixture was centrifuged (5 min, 8500 rpm) and filtered under vacuum, and the pellet was discarded. Acetone was evaporated under a nitrogen stream until the original volume of fermentation (2 L) to get the crude extract. This aqueous residue was loaded onto an SP207ss resin column (65 g, 32 × 100 mm) and eluted with an acetone–H<sub>2</sub>O stepped gradient (10/90 for 6 min, 20/80 for 6 min, 40/60 for 6 min, 60/40 for 6 min, 80/20 for 6 min, and 100/0 for 12 min, 10 mL/min, 20 mL/fraction) in a Teledyne CombiFlash RF instrument to give 21 fractions. Fraction 16 (obtained with 80% acetone) was subjected to preparative reversed-phase HPLC (Kinetex PFP Phenomenex, 21.2 × 250 mm, 5 μm, 14 mL/min, UV detection at 210 and 280 nm, 8.75 mL/fraction) using H<sub>2</sub>O (solvent A) and CH<sub>3</sub>CN (solvent B). Elution was carried out using isocratic conditions of 5% B for 5 min and then a linear gradient from 5% to 70% B in 52 min, yielding 73 fractions. Subfraction 38 was further purified by semipreparative reversed-phase HPLC (Zorbax RX-C<sub>8</sub>, 9.4 × 250 mm, 5 μm, 3.6 mL/min, UV detection at 210 and 280 nm, 1.8 mL/fraction) using H<sub>2</sub>O + 0.1% TFA (solvent A) and CH<sub>3</sub>CN + 0.1% TFA (solvent B). Elution was carried out using isocratic conditions of 25% B for 5 min followed by a linear gradient from 25% B to 75% B in 35 min to yield **1** (*t<sub>R</sub>* 24.5 min, 0.3 mg).

Fraction 17, also obtained with 80% acetone, was subjected to preparative reversed-phase HPLC under the same conditions used for fraction 16. Subfraction 41 was further purified using the conditions described above for subfraction 38 to yield **2** (*t<sub>R</sub>* 26 min, 0.5 mg) and **3** (*t<sub>R</sub>* 28 min, 0.5 mg).

**Krisynomycin B (1):** white amorphous solid;  $[\alpha]_D^{25}$  –15.8 (*c* 0.07, MeOH); UV (DAD) 210, 290 nm; IR (ATR)  $\nu_{\max}$  3074, 2966, 2927, 2870, 1623, 1593, 1532, 1510, 1434, 1240, 1203, 1182, 1134, 829 cm<sup>-1</sup>; <sup>1</sup>H and <sup>13</sup>C NMR data see Table 1; (+)-HRESIMS *m/z* 1331.5981 [M + H]<sup>+</sup> (calcd for C<sub>63</sub>H<sub>87</sub>N<sub>12</sub>O<sub>18</sub>S, 1331.5977).

**Krisynomycin C (2):** white amorphous solid;  $[\alpha]_D^{25}$  –2.1 (*c* 0.07, MeOH); UV (DAD) 210, 290 nm; IR (ATR)  $\nu_{\max}$  3076, 2968, 2924, 2867, 1669, 1622, 1593, 1532, 1510, 1434, 1239, 1203, 1181, 1134, 831 cm<sup>-1</sup>; <sup>1</sup>H and <sup>13</sup>C NMR data see Table 1; (+)-HRESIMS *m/z* 1365.5607 [M + H]<sup>+</sup> (calcd for C<sub>63</sub>H<sub>85</sub>ClN<sub>12</sub>O<sub>18</sub>S, 1365.5587).

**Krisynomycin (3):** white amorphous solid;  $[\alpha]_D^{25}$  –12.4 (*c* 0.13, MeOH); UV (DAD) 210, 290 nm; IR (ATR)  $\nu_{\max}$  3067, 2969, 2922, 2873, 1675, 1531, 1437, 1200, 1178, 1134, 837 cm<sup>-1</sup>; <sup>1</sup>H and <sup>13</sup>C NMR data see Table 1; (+)-HRESIMS *m/z* 1399.5206 [M + H]<sup>+</sup> (calcd for C<sub>63</sub>H<sub>84</sub>Cl<sub>2</sub>N<sub>12</sub>O<sub>18</sub>S, 1399.5197).

**Marfey's Analysis of Compound 1.** A sample (100 μg) of compound **1** was dissolved in 0.2 mL of 6 N HCl and heated at 110 °C for 16 h. The crude hydrolysate was evaporated to dryness under a N<sub>2</sub> stream, and the residue was dissolved in 100 μL of water. This solution was divided into two 50 μL aliquots. To each aliquot of the hydrolysate and to an aliquot (50 μL) of a 50 mM solution of each amino acid (D, L, or a DL mixture) were added 20 μL of a 1 M NaHCO<sub>3</sub> solution and a 1% (w/v) solution (100 μL) of D- or L-FDVA (Marfey's reagent, *N*-(2,4-dinitro-5-fluorophenyl)-L-valinamide). The reaction mixtures were incubated at 40 °C for 60 min. The reactions were quenched by addition of 20 μL of 1 N HCl, and the crude mixtures were diluted with 200 μL of acetonitrile and analyzed by LC/MS on an Agilent 1260 Infinity II single quadrupole LC/MS instrument. Separations were carried out on an Atlantis T3 column (4.6 × 100 mm, 5 μm) maintained at 40 °C. A mixture of two solvents, A (10% CH<sub>3</sub>CN, 90% H<sub>2</sub>O) and B (90% CH<sub>3</sub>CN, 10% H<sub>2</sub>O), both containing 1.3 mM trifluoroacetic acid and 1.3 mM ammonium formate, was used as the mobile phase under a linear gradient elution mode (isocratic 25% B for 2 min, 25–45% B in 27 min, isocratic 45% B for 5 min) at a flow rate of 1 mL/min.

Retention times (min) for the derivatized (D-FDVA) amino acid standards under the reported conditions were as follows: D-Cya: 2.74; L-Cya: 2.88, D-Ser: 4.32, L-Ser: 5.21, D-Ala: 7.16, L-Ala: 11.81, D-Pro: 7.75, L-Pro: 11.18, D-Val: 11.81, L-Val: 21.79, D-Leu: 16.20, L-Leu: 27.90, D-Trp: 16.20, L-Trp: 22.40. Retention times (min) for the observed peaks in the HPLC trace of the D-FDVA-derivatized

hydrolysis product of compound **1** were as follows: L-Cya: 2.99, L-Ser: 5.28, L-Pro: 11.21, L-Ala: 11.83, D-Val: 11.83, D-Leu: 16.33, and L-Val: 21.83.

**Genomic DNA Isolation, Sequencing, and Bioinformatic Analysis.** Genomic DNA of strain CA-091830 was extracted and purified as previously described from cultures grown in the same seed medium employed for the production of krisynomycins.<sup>49</sup> The genome of strain CA-091830 was sequenced and assembled de novo using a combined strategy of Illumina NovaSeq6000 S4 and PacBio sequencing (Macrogen, Seoul, Korea). Eleven contigs with a total length of 9 895 814 bp were obtained. Identification of potential BGCs was carried out with antiSMASH, and annotation of the ORFs was performed employing the translated sequences and the BLASTP algorithm at the NCBI Web site. The krisynomycins' BGC was analyzed using both antiSMASH<sup>22</sup> and PRISM.<sup>33</sup> Bioinformatic analysis of the condensation domains of the NRPS proteins KriF and KriG was carried out using a phylogenetic analysis employing their amino acid sequences together with the amino acid sequences of 525 known condensation domains.<sup>34</sup>

**Antibacterial Activity Bioassay.** MRSA COL MBS393 is a hospital-acquired penicillinase-negative strain widely used in *S. aureus* methicillin resistance and virulence studies. The broth dilution method was used to determine MIC values, and they were defined as the lowest concentration of compound that either singly or in combination with imipenem inhibited ≥90% of the growth of MRSA strain after overnight incubation. Bioassay was performed in triplicate on three different days. The antibacterial activities of the compounds were evaluated using sequential 2-fold serial dilutions in DMSO to provide 20 concentrations starting at 128 μg/mL for all the assays. The Genedata Screener software (Genedata, Inc., Basel, Switzerland) was used to process and analyze the data as well as to calculate the RZ factor, which predicts the robustness of the assay.<sup>50,51</sup> The RZ factor obtained from all experiments ranged between 0.90 and 0.97.

The MRSA COL MB 5393 strain was grown in a shaken culture (220 rpm) of brain heart infusion broth (BHI, 37 g/L) incubated overnight at 37 °C. The bacterial inoculum was then diluted to obtain the corresponding equivalent for the assay of approximately 1.1 × 10<sup>6</sup> CFU/mL. For the assay, 90 μL/well of diluted inoculum was mixed with 1.6 μL/well of each compound dissolved in DMSO and 8.4 μL/well of four different concentrations of imipenem starting at 4 μg/mL (subminimal inhibitory concentration). Vancomycin was included as positive control on each plate. The absorbance at *T*<sub>0</sub> (zero time) was measured at 612 nm with an EnVision multimode plate spectrophotometer, and immediately thereafter, the plates were incubated at 37 °C for 18 h. After this period, the assay plates were shaken using a Micromix-5 agitator, and once again the absorbance at *T*<sub>f</sub> (final time) was measured at 612 nm. The percentage of growth inhibition was calculated according to previously described methodology.<sup>52</sup>

## ■ ASSOCIATED CONTENT

### Supporting Information

The Supporting Information is available free of charge at <https://pubs.acs.org/doi/10.1021/acs.jnatprod.0c00294>.

1D and 2D NMR spectra and MS/MS fragmentation data of krisynomycins, together with HPLC chromatograms of Marfey's analysis of compound **1** and additional information on the biosynthetic pathway (PDF)

## ■ AUTHOR INFORMATION

### Corresponding Authors

Mercedes Pérez-Bonilla – Fundación MEDINA, Centro de Excelencia en Investigación de Medicamentos Innovadores en Andalucía, 18016 Armilla, Granada, Spain; Phone: +34 958993965; Email: [mercedes.perez@medinaandalucia.es](mailto:mercedes.perez@medinaandalucia.es)

Fernando Reyes – Fundación MEDINA, Centro de Excelencia en Investigación de Medicamentos Innovadores en Andalucía,

18016 Armilla, Granada, Spain; [orcid.org/0000-0003-1607-5106](https://orcid.org/0000-0003-1607-5106); Phone: +34 958993965, ext. 7006;  
Email: fernando.reyes@medinaandalucia.es

## Authors

**Daniel Oves-Costales** – Fundación MEDINA, Centro de Excelencia en Investigación de Medicamentos Innovadores en Andalucía, 18016 Armilla, Granada, Spain

**Ignacio González** – Fundación MEDINA, Centro de Excelencia en Investigación de Medicamentos Innovadores en Andalucía, 18016 Armilla, Granada, Spain

**Mercedes de la Cruz** – Fundación MEDINA, Centro de Excelencia en Investigación de Medicamentos Innovadores en Andalucía, 18016 Armilla, Granada, Spain

**Jesús Martín** – Fundación MEDINA, Centro de Excelencia en Investigación de Medicamentos Innovadores en Andalucía, 18016 Armilla, Granada, Spain

**Francisca Vicente** – Fundación MEDINA, Centro de Excelencia en Investigación de Medicamentos Innovadores en Andalucía, 18016 Armilla, Granada, Spain

**Olga Genilloud** – Fundación MEDINA, Centro de Excelencia en Investigación de Medicamentos Innovadores en Andalucía, 18016 Armilla, Granada, Spain

Complete contact information is available at:

<https://pubs.acs.org/10.1021/acs.jnatprod.0c00294>

## Notes

The authors declare no competing financial interest.

## ACKNOWLEDGMENTS

The polarimeter, HPLC, IR, and NMR equipment, and plate reader used in this work were purchased via grants for scientific and technological infrastructures from the Ministerio de Ciencia e Innovación [Grant Nos. PCT-010000-2010-4 (NMR), INP-2011-0016-PCT-010000 ACT6 (polarimeter, HPLC, and IR), and PCT-01000-ACT7, 2011-13 (plate reader)].

## REFERENCES

- (1) World Health Organization. Key Facts, 2018 (accessed March 17, 2020) <http://www.who.int/news-room/fact-sheets/detail/antimicrobial-resistance>.
- (2) Harbarth, S.; Balkhy, H. H.; Goossens, H.; Jarlier, V.; Kluytmans, J.; Laxminarayan, R.; Saam, M.; Van Belkum, A.; Pittet, D. *Antimicrob. Resist. Infect. Control* **2015**, *4*, 49.
- (3) O'Neill, J. Antimicrobial Resistance: Tackling a crisis for the health and wealth of nations. The Review on Antimicrobial Resistance chaired by Jim O'Neill. December 2014 (accessed March 17, 2020); [https://amr-review.org/sites/default/files/AMR%20Review%20Paper%20-%20Tackling%20a%20crisis%20for%20the%20health%20and%20wealth%20of%20nations\\_1.pdf](https://amr-review.org/sites/default/files/AMR%20Review%20Paper%20-%20Tackling%20a%20crisis%20for%20the%20health%20and%20wealth%20of%20nations_1.pdf).
- (4) Bérdy, J. *J. Antibiot.* **2005**, *58*, 1–26.
- (5) Newman, D. J.; Cragg, G. M. *J. Nat. Prod.* **2016**, *79*, 629–661.
- (6) Baltz, R. H. *Curr. Opin. Pharmacol.* **2008**, *8*, 557–563.
- (7) Genilloud, O. *Nat. Prod. Rep.* **2017**, *34*, 1203–1232.
- (8) Abdalla, M. A.; McGaw, L. J. *Molecules* **2018**, *23*, 2080.
- (9) Larrull, L. I.; Testero, S. A.; Fisher, J. F.; Mobashery, S. *Curr. Opin. Microbiol.* **2010**, *13*, 551–557.
- (10) Peacock, S. J.; Paterson, G. K. *Annu. Rev. Biochem.* **2015**, *84*, 577–601.
- (11) Foster, T. J. *Trends Microbiol.* **2019**, *27*, 26–38.
- (12) Therien, A. G.; Huber, J. L.; Wilson, K. E.; Beaulieu, P.; Caron, A.; Claveau, D.; Deschamps, K.; Donald, R. G.; Galgocsi, A. M.; Gallant, M.; Gu, X.; Kevin, N. J.; Lafleur, J.; Leavitt, P. S.; Lebeau-

Jacob, C.; Lee, S. S.; Lin, M. M.; Michels, A. A.; Ogawa, A. M.; Painter, R. E.; Parish, C. A.; Park, Y.-W.; Benton-Perdomo, L.; Petcu, M.; Phillips, J. W.; Powles, M. A.; Skorey, K. I.; Tam, J.; Tan, C. M.; Young, K.; Wong, S.; Waddell, S. T.; Miesel, L. *Antimicrob. Agents Chemother.* **2012**, *56*, 4662–4670.

(13) Fukumoto, A.; Kim, Y.-P.; Hanaki, H.; Shiomi, K.; Tomoda, H.; Omura, S. *J. Antibiot.* **2008**, *61*, 7–10.

(14) Koyama, N.; Tokura, Y.; Takahashi, Y.; Tomoda, H. *Acta Pharm. Sin. B* **2011**, *1*, 236–239.

(15) Yamazaki, H.; Omura, S.; Tomoda, H. *J. Antibiot.* **2010**, *63*, 329–330.

(16) Fischbach, M. A.; Walsh, C. T. *Chem. Rev.* **2006**, *106*, 3468–3496.

(17) Sinha, S.; Nge, C.-E.; Leong, C. Y.; Ng, V.; Crasta, S.; Alfatah, M.; Goh, F.; Low, K.-N.; Zhang, H.; Arumugam, P.; Lezhava, A.; Chen, S. L.; Kanagasundaram, Y.; Ng, S. B.; Eisenhaber, F.; Eisenhaber, B. *BMC Genomics* **2019**, *20*, 374.

(18) Marfey, P. *Carlsberg Res. Commun.* **1984**, *49*, 591–596.

(19) Muramoto, K.; Kamiya, H. *Anal. Biochem.* **1990**, *189*, 223–230.

(20) Matsubara, H.; Sasaki, R. M. *Biochem. Biophys. Res. Commun.* **1969**, *35*, 175–181.

(21) Yokote, Y.; Murayama Arai, K.; Akahane, K. *Anal. Biochem.* **1986**, *152*, 245–249.

(22) Blin, K.; Shaw, S.; Steinke, K.; Villebro, R.; Ziemert, N.; Lee, S. Y.; Medema, M. H.; Weber, T. *Nucleic Acids Res.* **2019**, *47*, W81–W87.

(23) Amoutzias, G. D.; Van de Peer, Y.; Mossialos, D. *Future Microbiol.* **2008**, *3*, 361–370.

(24) Graham, D. E.; Taylor, S. M.; Wolf, R. Z.; Namboori, S. C. *Biochem. J.* **2009**, *424*, 467–478.

(25) Wang, M.; Chen, D.; Zhao, Q.; Liu, W. *J. Org. Chem.* **2018**, *83*, 7102–7108.

(26) Yeh, E.; Garneau, S.; Walsh, C. T. *Proc. Natl. Acad. Sci. U. S. A.* **2005**, *102*, 3960–3965.

(27) Wu, C.; Du, C.; Gubbens, J.; Choi, Y. H.; van Wezel, G. P. *J. Nat. Prod.* **2015**, *78*, 2355–2363.

(28) Takahashi, S.; Takagi, H.; Toyoda, A.; Uramoto, M.; Nogawa, T.; Ueki, M.; Sakaki, Y.; Osada, H. *J. Bacteriol.* **2010**, *192*, 2839–2851.

(29) Ozaki, T.; Nishiyama, M.; Kuzuyama, T. *J. Biol. Chem.* **2013**, *288*, 9946–9956.

(30) Roose, B. W.; Christianson, D. W. *Biochemistry* **2019**, *58*, 3232–3242.

(31) Unsöld, I. A.; Li, S.-M. *Microbiology* **2005**, *151*, 1499–1505.

(32) Ding, Y.; Williams, R. M.; Sherman, D. H. *J. Biol. Chem.* **2008**, *283*, 16068–16076.

(33) Skinnider, M. A.; Merwin, N. J.; Johnston, C. W.; Magarvey, N. A. *Nucleic Acids Res.* **2017**, *45*, W49–W54.

(34) Rausch, C.; Hoof, I.; Weber, T.; Wohlleben, W.; Huson, D. H. *BMC Evol. Biol.* **2007**, *7*, 78.

(35) Hernandez, M. Z.; Cavalcanti, S. M. T.; Moreira, D. R. M.; de Azevedo Junior, W. F.; Leite, A. C. L. *Curr. Drug Targets* **2010**, *11*, 303–314.

(36) Tello, M.; Kuzuyama, T.; Heide, L.; Noel, J. P.; Richard, S. B. *Cell. Mol. Life Sci.* **2008**, *65*, 1459–1463.

(37) Tanner, M. E. *Nat. Prod. Rep.* **2015**, *32*, 88–101.

(38) Memic, A.; Spaller, M. R. *ChemBioChem* **2008**, *9*, 2793–2795.

(39) van Pée, K.-H.; Patallo, E. P. *Appl. Microbiol. Biotechnol.* **2006**, *70*, 631–641.

(40) Zhu, X.; De Laurentis, W.; Leang, K.; Herrmann, J.; Ihlefeld, K.; van Pée, K.-H.; Naismith, J. H. *J. Mol. Biol.* **2009**, *391*, 74–85.

(41) Feling, R. H.; Buchanan, G. O.; Mincer, T. J.; Kauffman, C. A.; Jensen, P. R.; Fenical, W. *Angew. Chem., Int. Ed.* **2003**, *42*, 355–357.

(42) Martín, J.; Crespo, G.; González-Menéndez, V.; Pérez-Moreno, G.; Sánchez-Carrasco, P.; Pérez-Victoria, I.; Ruiz-Pérez, L. M.; González-Pacanoska, D.; Vicente, F.; Genilloud, O.; Bills, G. F.; Reyes, F. *J. Nat. Prod.* **2014**, *77*, 2118–2123.

(43) Hayakawa, M.; Otaguro, M.; Takeuchi, T.; Yamazaki, T.; Iimura, Y. *Antonie van Leeuwenhoek* **2000**, *78*, 171–185.

- (44) Yoon, S. H.; Ha, S. M.; Kwon, S.; Lim, J.; Kim, Y.; Seo, H.; Chun, J. *Int. J. Syst. Evol. Microbiol.* **2017**, *67*, 1613–1617.
- (45) Tamura, K.; Stecher, G.; Peterson, D.; Filipski, A.; Kumar, S. *Mol. Biol. Evol.* **2013**, *30*, 2725–2729.
- (46) Thompson, J. D.; Gibson, T. J.; Plewniak, F.; Jeanmougin, F.; Higgins, D. G. *Nucleic Acids Res.* **1997**, *25*, 4876–4882.
- (47) Saitou, N.; Nei, M. *Mol. Biol. Evol.* **1987**, *4*, 406–425.
- (48) Jukes, T. H.; Cantor, C. *Evolution of Protein Molecules, in Mammalian Protein Metabolism*; Academic Press, 1969.
- (49) Kieser, T.; Bibb, M. J.; Buttner, M. J.; Chater, K. F.; Hopwood, D. A. *Preparation and Analysis of Genomic and Plasmid DNA in Practical Streptomyces Genetics*; John Innes Foundation, Norwich, 2000.
- (50) Zhang, J. H.; Chung, T. D.; Oldenburg, K. R. *J. Biomol. Screening* **1999**, *4*, 67–73.
- (51) Kümmel, A.; Gubler, H.; Gehin, P.; Beibel, M.; Gabriel, D.; Parker, C. N. *J. Biomol. Screening* **2010**, *15*, 95–101.
- (52) Martín, J.; da S. Sousa, T.; Crespo, G.; Palomo, S.; González, I.; Tormo, J. R.; de la Cruz, M.; Anderson, M.; Hill, R. T.; Vicente, F.; Genilloud, G.; Reyes, F. *Mar. Drugs* **2013**, *11*, 387–398.